

地下水丘模擬：(I). 理論推導及討論

Simulation of Ground Water Mounding:

(I). Theoretical Derivation and Discussion— Technical Note

台大水工所博士後副研究員

蔡存孝

Tswn-Syau Tsay

美國威斯康辛大學

麥迪遜分校土木環工系教授

John Hoopes

美國密西西比大學工程研究中心研究員

江明義

Min-Yee Jiang

摘要

本文利用一般非直角系座標模擬地下水丘以解決其所產生之自由及移動邊界問題。非直角系座標下之控制方程式以張量表之，因此，因為變形而產生之效應可被考慮。計算過程包括製造格子點、將直角系座標 (physical domain) 轉成非直角系座標 (computational domain)、最後在非直角系座標下解問題，而得到精確且合理之關鍵在於格子點。本文推導出 poisson type equation 在非直角系座標下之張量形式，其用 Hele-Shaw Model 驗證之結果將於下篇文章敘述之。

關鍵詞：地下水丘，張量，自由及移動邊界。

ABSTRACT

Simulation of ground water mounding uses the computation in the generalized curvilinear coordinate to resolve the free and moving boundary problem. The general form of governing equation and boundary conditions of the curvilinear coordinate are presented by tensor so that the stretching and the rotation and/or angular deformation effects can be accounted. The procedure involves generating a grid in the physical domain, then transforming the physical domain (Cartesian coordinate) into the computational domain (generalized curvilinear coordinate), and finally solving the problem in the computational domain. Grid generation for the physical domain is a key step to obtain accurate, reasonable solutions. This paper derived a complete tensor form of the generalized curvilinear coordinate for a poisson type equation. The verification by Hele-Shaw model is stated in the following paper.

Keywords : Ground water mounding, Tensor, Free and moving boundary.

1. Literature review

There are two problems in determining ground water mounding computationally. One is to locate the free surface (water table) with local recharge. This boundary must be known in order to compute the flow field due to mounding. On the other hand, the flow field also influences the location of the free surface. Consequently, the determination of the free surface location has to be solved by an iteration scheme. Further, as the computational grid in a numerical scheme using finite differences generally is fixed and as the free surface location changes from one iteration to the next, the final computed free surface position will be approximate as the free surface is not located exactly on grid points.

Ground water mounding had been known for many years. Different approaches have been used to account for heterogeneity, unknown free surface position, non-linear conditions, and irregular geometry. It is common to assume that an aquifer is homogeneous or has a hydraulic conductivity varying with depth or horizontal location according to known functions. Steady-state analytical solutions, assuming the aquifer is homogeneous, were found for models with simple geometry, based on the Dupuit-Forchheimer assumption (Haar, 1962; Huisman, 1972). These assumptions also have been used to develop unsteady-state solutions (Hantush, 1967; Huisman, 1972; Maasland and Bittinger, 1963; Marino, 1974). The Dupuit-Forchheimer theory was used to solve a three-dimensional problem by Strack (1984) in which the flow field in three-dimensions is obtained using the incompressibility condition and two-dimensional Dupuit-Forchheimer flow models. Youngs (1965) applied the Grinskii (1964) discharge potential to obtain an estimate of the error of solutions for cases with hydraulic conductivity varying with depth.

Some other analytical approaches have employed a linearization of the non-linear free surface boundary condition. Dagan (1967) developed solutions derived by an expansion in a small parameter that linearizes the

exact equations of flow. Using Dupuit-Forchheimer and potential theories, Brock (1976) presented solutions for ground water mounding with both linear and nonlinear boundary conditions. An exact solution was found for the linearized case applied on the original, undisturbed water table; a numerical solution by finite differences was used for the nonlinear case. Schmitz and Edenhofer (1988) presented a semi-analytical solution for ground water mounding using conformal mapping and the theory of complex functions.

Application of the spectral method has been used to solve ground water mounding. Kirkham and Powers (1964) used this method to obtain an exact theoretical solution for flow through a homogeneous, rectangular block of soil with constant heads on each boundary, including the seepage face. The solution obtains the coefficients and the water table height by matching the water table's stream function and potential function at a finite number of points. Murray (1970) solved the same model as Kirkham and Powers (1964) did by applying a spline function. A trial and error method was used to find the right position for calculating the water table. He also indicated that Kirkham's method does not converge to the seepage face height. The author has applied the spectral method in conjunction with the Grinskii discharge potential to simulate the flow field due to mounding in a simple homogeneous aquifer; however, no reasonable solution was obtained.

Finite differences have also been used to solve such problems. Singh (1976) applied finite differences with a simple transformation to linearize the free surface boundary condition. His model requires a reasonable initial guess for the free surface. In some cases, the predicted location of the water table may not be accurate, and a number of iterations are required to arrive at a satisfactory solution in each step. This condition is mainly due to the fact that the free surface boundary is not located on grid points. Another popular numerical ground water model is MODFLOW (1988) (A Modular Three-Dimensional Finite-Difference Ground-Water Flow Model), which can be used to simulate three-

dimensional ground water flows in unconfined and confined aquifers with heterogeneous or homogeneous media. As the model applies mass conservation to rectangular blocks of various sizes, its flow field resolution is limited when the flow domain and heterogeneity geometry are of a scale equal to or smaller than the block size.

The boundary integral equation method has been used to solve free surface problems by Liggett and Hadjitheodorou (1965). The Lagrangian dynamical equations were used to solve the flow field following rapid drawdown adjacent to a steep earth embankment. By the same method, Liggett (1977) presented a solution for the free surface position without recharge. Liu and Liggett(1979) used the same idea to solve for ground water mounding. Solutions for a three-dimensional potential flow problem in an unconfined aquifer was presented three years later (Lennon et al., 1980).

In the development of aerospace engineering, conformal mapping has played an important role. The basic idea of conformal mapping is to transform an arbitrary contour into a circle using analytical functions so that problems of potential flow can be solved; this method utilizes the invariance of solutions to Laplace's equation mapped by analytic functions. This technique is suitable and efficient; yet applications to fluid dynamics were rare before 1970's because of the computational difficulties (Fletcher, 1991). Conformal mapping was also applied in the field of ground water mechanics. Many closed-form solutions for simplified ground water flow problems were developed before computers were widely used (Harr,1962).

The field of computational fluid dynamics has rapidly developed with the use of computers. Since the computational difficulties can be overcome, the equations of motion can be solved numerically considering pressure, viscous shear and compressibility. To undertake accurate calculations, a well-organized computational grid is necessary. In the early 1970's the theory of numerically-generated, boundary-conforming coordinate systems was developed in order to meet the

need for a well-organized grids of arbitrarily-shaped geometry. From that time on, many sophisticated automatic grid generation codes, such as INMESH, WESCOR (two-dimensional), and EAGLE,EagleView, and GRIDGEN (three-dimensional), have been developed (Thompson, et al., 1985).

2. Transformation relationships

2.1 Coordinate transform

For the finite difference method, the imposition of boundary conditions on a domain of complex geometry requires a complicated interpolation of the data on local grid lines (such as Singh, 1976) and typically, a local loss of accuracy in the computational solution. Such difficulties motivated the introduction of a mapping or transformation from the physical domain (x,y,z)(rectangular coordinate domain)to a computational domain (ξ , η , ζ)(generalized coordinate domain). A distorted region in the physical domain is mapped into a rectangular region in generalized coordinate space (Fig. 1).

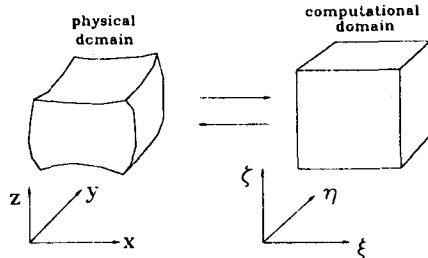


Fig. 1 Correspondence of the physical and generalized coordinate domain

It is assumed that there is a unique, single-valued relation between the physical domain and the generalized coordinate domain; for a three-dimensional problem, these relations are

$$\xi = \xi (x,y,z) , \quad (1a)$$

$$\eta = \eta (x,y,z) \text{ and } \quad (1b)$$

$$\zeta = \zeta (x,y,z) \quad (1c)$$

with the inverse relations

$$x = x(\xi , \eta , \zeta) , \quad (2a)$$

$$y = y(\xi , \eta , \zeta) \text{ and } \quad (2b)$$

$$z = z(\xi , \eta , \zeta) \quad (2c)$$

The Jacobian matrix, J, and its inverse, J^{-1} for

these relations are

$$\underline{J} = \begin{bmatrix} \frac{\partial \xi}{\partial x} & \frac{\partial \xi}{\partial y} & \frac{\partial \xi}{\partial z} \\ \frac{\partial \eta}{\partial x} & \frac{\partial \eta}{\partial y} & \frac{\partial \eta}{\partial z} \\ \frac{\partial \zeta}{\partial x} & \frac{\partial \zeta}{\partial y} & \frac{\partial \zeta}{\partial z} \end{bmatrix} \quad (3)$$

and

$$\underline{J}^{-1} = \begin{bmatrix} \frac{\partial x}{\partial \xi} & \frac{\partial x}{\partial \eta} & \frac{\partial x}{\partial \zeta} \\ \frac{\partial y}{\partial \xi} & \frac{\partial y}{\partial \eta} & \frac{\partial y}{\partial \zeta} \\ \frac{\partial z}{\partial \xi} & \frac{\partial z}{\partial \eta} & \frac{\partial z}{\partial \zeta} \end{bmatrix} \quad (4)$$

The elements of \underline{J}^{-1} can be related to the elements of \underline{J} by

$$\underline{J} = \frac{\text{Transpose of Cofactor}(\underline{J}^{-1})}{|\underline{J}^{-1}|}$$

where

$$|\underline{J}^{-1}| = x_{\xi}(y_{\eta}z_{\zeta} - y_{\zeta}z_{\eta}) - x_{\eta}(y_{\xi}z_{\zeta} - y_{\zeta}z_{\xi}) + x_{\zeta}(y_{\xi}z_{\eta} - y_{\eta}z_{\xi}) \quad (6)$$

Using Equations (5) and (6) the elements of \underline{J} in (3) can be expressed as

$$\xi_x = \frac{y_{\eta}z_{\zeta} - y_{\zeta}z_{\eta}}{|\underline{J}^{-1}|}, \quad (7a)$$

$$\xi_y = \frac{x_{\zeta}z_{\eta} - x_{\eta}z_{\zeta}}{|\underline{J}^{-1}|}, \quad (7b)$$

$$\xi_z = \frac{x_{\eta}y_{\zeta} - x_{\zeta}y_{\eta}}{|\underline{J}^{-1}|}, \quad (7c)$$

$$\eta_x = \frac{y_{\zeta}z_{\xi} - y_{\xi}z_{\zeta}}{|\underline{J}^{-1}|}, \quad (7d)$$

$$\eta_y = \frac{x_{\xi}z_{\zeta} - x_{\zeta}z_{\xi}}{|\underline{J}^{-1}|}, \quad (7e)$$

$$\eta_z = \frac{x_{\zeta}y_{\xi} - x_{\xi}y_{\zeta}}{|\underline{J}^{-1}|}, \quad (7f)$$

$$\zeta_x = \frac{y_{\xi}z_{\eta} - y_{\eta}z_{\xi}}{|\underline{J}^{-1}|}, \quad (7g)$$

$$\zeta_y = \frac{x_{\eta}z_{\xi} - x_{\xi}z_{\eta}}, \quad \text{and} \quad (7h)$$

$$\zeta_z = \frac{x_{\xi}y_{\eta} - x_{\eta}y_{\xi}}{|\underline{J}^{-1}|} \quad (7i)$$

Another matrix, g , used in the governing equation and boundary conditions, is

$$\underline{g} = \begin{bmatrix} g_{11} & g_{12} & g_{13} \\ g_{21} & g_{22} & g_{23} \\ g_{31} & g_{32} & g_{33} \end{bmatrix}, \quad (8)$$

where

$$g_{ij} = \sum_{k=1}^3 \frac{\partial x^k}{\partial \xi^i} \frac{\partial x^k}{\partial \xi^j} \quad (9)$$

The above equations are used to transform the governing and boundary conditions from the physical domain to the computational domain.

2.2 Evaluation of transformation relations

Numerical implementation of the transformation Eqs. ((7)-(9)) is carried out using second order central differences. Thus, for the interior point (I,J,K)

$$x_{\xi} = \frac{x_{i+1,j,k} - x_{i-1,j,k}}{\xi_{i+1,j,k} - \xi_{i-1,j,k}} \quad (10)$$

Points on the boundary also are evaluated by a second order approximation. When the domain is to the right of the boundary ($I=1$), z_{ξ} is

$$z_{\xi} = \frac{-3x_{1,j,k} + 4x_{2,j,k} - x_{3,j,k}}{\xi_{3,j,k} - \xi_{1,j,k}} \quad (11)$$

In computation, the grid spacing in the computational domain is taken to be unity. Hence, Eqs. (10) and (11) are rewritten

$$x_{\xi} = \frac{x_{i+1,j,k} - x_{i-1,j,k}}{2} \quad (\text{for internal points}) \quad \text{and} \quad (12)$$

$$z_{\xi} = \frac{-3x_{1,j,k} + 4x_{2,j,k} - x_{3,j,k}}{2} \quad (\text{for points on the left boundary}). \quad (13)$$

Evaluations of the other derivatives are carried out in the same manner. Second-order transformation parameters are required when a second-order equation (e.g., Laplace's equation) is transformed into the generalized curvilinear coordinate. For example,

$$x_{\xi\xi} = x_{i+1,j,k} - 2x_{i,j,k} + x_{i-1,j,k}, \quad (14a)$$

$$x_{\eta\eta} = x_{i,j+1,k} - 2x_{i,j,k} + x_{i,j-1,k} \quad \text{and} \quad (14b)$$

$$x_{\xi\eta} = \frac{x_{i+1,j+1,k} + x_{i-1,j-1,k} - x_{i+1,j-1,k} - x_{i-1,j+1,k}}{4} \quad (14c)$$

In a similar way, other second-order parameters can be evaluated.

3. Grid generation

The computational grids in this work were generated by EagleView, developed at Mississippi State University. This software must be run on a Silicon Graphics Computer. It is a panel controlling code. The theoretical part of EagleView is described by Thompson

et al. (1985). General rules for generating grids are based upon the following considerations.

3.1 Limitation of memory

A dense, computational grid (small grid spacing) has less truncation error than a sparse grid but requires more memory. As each computer has a certain memory, the total number of grid points for modeling is limited. Thus, the number and distribution of the computational grid points are keys to obtaining reasonable and satisfactory results.

3.2 Point distribution

Because of the memory limitation, non-uniform grid points are frequently used. Truncation errors result from the grid spacing and the distribution function, which controls the smoothness of the grid. A one-dimensional, point distribution function, F_1 , can be written as

$$x(\xi) = F_1 \left[\frac{\xi}{N} \right], \text{ where } 0 \leq \xi \leq N \quad (15)$$

Suppose x varies from 0 to 1. The first derivative in one dimension of a function, $f(x)$, is

$$f_x = \frac{f_\xi}{x_\xi} \quad (16)$$

Using the central difference approximation of f_x , Eq.(16) can be written

$$f_x = \frac{1}{x_\xi} \left[\frac{f_{i+1} - f_{i-1}}{2\Delta\xi} \right] + T_1, \quad (17)$$

where T_1 is the truncation error. In this analysis, x_ξ is evaluated analytically. Therefore, there is no truncation error for this term (Effect of numerical metric coefficients is discussed by Thompson et al., 1985). Using a Taylor series expansion for f_{i+1} and f_{i-1} on ξ_0 gives

$$f(\xi_0 \pm \Delta\xi) = f(\xi_0) \pm \Delta\xi f_\xi(\xi_0) + \frac{1}{2!} \Delta\xi^2 f_{\xi\xi}(\xi_0) \pm \frac{1}{3!} \Delta\xi^3 f_{\xi\xi\xi}(\xi_0) + \dots \quad (18)$$

Letting $\Delta\xi = 1$ and substituting Eqs. (18) into Eq. (17), T_1 is

$$T_1 = -\frac{1}{3!} \frac{f_{\xi\xi\xi}}{x_\xi} - \frac{1}{5!} \frac{f_{\xi\xi\xi\xi\xi}}{x_\xi} \dots \quad (19)$$

Even though ξ -derivatives of f describe a point distribution, Eq. (19) can not be truncated since ξ -derivatives of f are dependent on the point distribution.

ξ -derivatives of f change with the change of number of points (N) or distribution function (F_1). Hence, the truncation error can not be expressed in terms of ξ -derivatives of f ; however, the ξ -derivatives are transformed to x -derivatives for further discussion. From Eq.(16)

$$f_{\xi\xi} = x_{\xi\xi} f_x + x_\xi (f_x)_\xi = x_{\xi\xi} f_x + x_\xi^2 f_{xx} \text{ and} \quad (20)$$

$$f_{\xi\xi\xi} = x_{\xi\xi\xi} f_x + 3x_{\xi\xi} x_\xi f_{xx} + x_\xi^3 f_{xxx} \quad (21)$$

(A) Fixed distribution function

Consider changing the number of points (N) with a fixed distribution function. From Eq. (15)

$$x_\xi = \frac{F_1'}{N}, \quad x_{\xi\xi} = \frac{F_1''}{N^2}, \quad x_{\xi\xi\xi} = \frac{F_1'''}{N^3} \quad (22)$$

From (20),(21),and(22),it is clear that

$$f_{\xi\xi\xi} \propto N^{-3}, \text{ and } f_{\xi\xi\xi\xi\xi} \propto N^{-5} \quad (23)$$

The second term in T_1 , Eq.(19), can be neglected because of Eq.(23). Substituting Eq.(21) into the first term of Eq.(19) gives

$$T_1 = -\frac{1}{6} \frac{x_{\xi\xi\xi} f_x}{x_\xi} - \frac{1}{2} x_{\xi\xi} f_{xx} - \frac{1}{6} x_\xi^2 f_{xxx} \quad (24)$$

Thus, from Eqs.(20) to (24) the truncation error (T_1) is proportional to N^{-2} .

(B) Fixed number of points

Since the number of points is fixed, the grid spacing must increase in some places, when it is decreased in other places. Hence, the truncation error depends upon the distribution function. As discussed by Thompson et al. (1985), the estimation is still not attainable.

3.3 Orthogonality

Consider orthogonality for a two-dimensional problem. The first derivative of $f(x)$ is given by

$$f_x = (y_\eta f_\eta - y_\xi f_\eta) / \sqrt{g}, \quad (25)$$

where $\sqrt{g} = |J^{-1}| = x_\xi y_\eta - x_\eta y_\xi$ (Eq.(6)).

With a two-point central difference for all derivatives (similar process described in the previous section), the leading term of the truncation error is

$$T_x = \frac{1}{2\sqrt{g}} (y_\xi x_\eta x_{\eta\eta} - x_\xi y_\eta x_{\xi\xi}) f_{xx} + \frac{1}{2\sqrt{g}} (y_\xi y_\eta) (y_{\eta\eta} - y_{\xi\xi}) f_{xy} + \frac{1}{2\sqrt{g}} [y_\xi y_\eta (x_{\eta\eta} - x_{\xi\xi}) + x_\eta y_\xi y_{\eta\eta} - x_\xi y_\eta y_{\xi\xi}] f_{xy} + \text{second order terms}, \quad (26)$$

where x_ξ, x_η, y_ξ and y_η are defined by Eq. (12) using central difference, and $x_{\xi\xi}$ and $x_{\eta\eta}$ are defined in Eqs. (14a) and (14b). The contribution from non-orthogonality can be considered with the case of skewed parallel lines with $x_\eta = x_{\eta\eta} = x_{\xi\eta} = y_{\xi\xi} = y_{\xi\eta} = 0$ (see Fig.(2)):

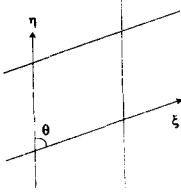


Fig. 2 Skewed parallel lines system

Hence, Eq. (25) can be reduced to

$$T_x = -\frac{1}{2}x_{\xi\xi}f_{xx} + \frac{1}{2}\left[\frac{y_\xi}{x_\xi}\right]y_{\eta\eta}f_{yy} - \frac{1}{2}\left[\frac{y_\xi}{x_\xi} - x_{\xi\xi}f_{yy}\right] \quad (27)$$

Since $\cot \theta = \frac{y_\xi}{x_\xi}$, Eq. (27) becomes

$$T_x = -\frac{1}{2}x_{\xi\xi}f_{xx} + \frac{1}{2}(y_{\eta\eta}f_{yy} - x_{\xi\xi}f_{yy})\cot \theta. \quad \text{(Thompson et al., 1985)} \quad (28)$$

Even if the grid is orthogonal, the first term still exists. However, an orthogonal or nearly orthogonal grid is preferred.

4. Governing equation and boundary conditions

4.1 Governing equation in generalized curvilinear coordinates

Introduction to tensors and tensor analysis are available in many books (Aris, 1962; Thompson et al., 1985; and Bird et al., 1987; etc.). Generalized curvilinear coordinates are related to Cartesian coordinates by Eqs. (1) and (2). In tensor notation, a point in Cartesian coordinates is given by x_i (x_1, x_2, x_3) and in generalized curvilinear coordinates is given by ξ^i (ξ^1, ξ^2, ξ^3). The directed line segment dr , joining two points an incremental distance apart (Fig. 3), is written

$$dr = \sum_i g_i d\xi^i, \quad (29)$$

which defines the base vector, g_i , in curvilinear coordinates. Thus

$$g_i = \frac{\partial}{\partial \xi^i} r = \sum_j \frac{\partial x_j}{\partial \xi^i} \frac{\partial}{\partial x_j} r = \sum_j \frac{\partial x_j}{\partial \xi^i} \delta_j, \quad (30)$$

where g_i and δ_j are covariant base vectors in curvilinear and Cartesian coordinates, respectively. g_i can be written as a linear combination of δ_j , are tangent to the coordinate curves but are not of unit length.

As the covariant base vectors are not necessarily

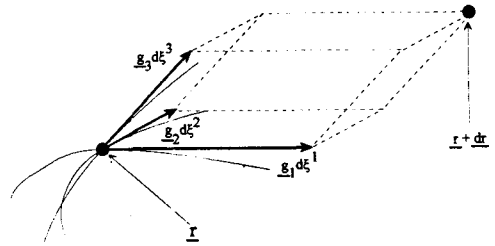


Fig. 3 Base vectors, g_i , in generalized curvilinear coordinates (Bird et al., 1987)

orthogonal in generalized curvilinear coordinates, contravariant base vectors, g^i , are introduced by

$$g^i = \nabla \xi^i = \sum_j \frac{\partial \xi^i}{\partial x_j} \delta_j, \quad (31)$$

The contravariant vectors, g^i , are perpendicular to the surface $\xi^i = \text{constant}$. From Eqs. (30) and (31),

$$g^i \cdot g_j = \delta_j^i \quad \text{and} \quad (32a)$$

$$g_i \cdot g^j = \delta_i^j, \quad (32b)$$

where δ_i^j is the Kronecker delta, which is 0 if $i \neq j$ and 1 if $i = j$. The covariant metric tensor is defined by

$$g_i \cdot g_j = g_{ij}, \quad (33a)$$

and the contravariant metric tensor is given by

$$g^i \cdot g^j = g^{ij}. \quad (33b)$$

The determinant of g_{ij} is called g ; $\sqrt{g} = g_1 \cdot (g_2 \times g_3) = \|J^{-1}\|$ (see Eq.(6)). The cross (vector) product of any two base vectors is

$$g_i \times g_j = \sum_k \sqrt{g} \epsilon_{ijk} g^k \quad \text{or} \quad (34a)$$

$$g^i \times g^j = \sum_k \frac{1}{\sqrt{g}} \epsilon_{ijk} g_k, \quad (34b)$$

where $\epsilon_{ijk} = 1$, if $ijk = 123, 231, 312$; $\epsilon_{ijk} = -1$, if $ijk = 321, 132, 213$; and $\epsilon_{ijk} = 0$, if any two indices are the same. The contravariant metric tensor can be evaluated from the covariant metric tensor as

$$g^{ij} = g^i \cdot g^j = \frac{1}{g} [g_j \times g_k] \cdot [g_m \times g_n] \\ = \frac{1}{g} [g_{jm}g_{kn} - g_{jn}g_{km}], \quad (35)$$

using the identity

$$\begin{aligned} (\mathbf{A} \times \mathbf{B}) \cdot (\mathbf{C} \times \mathbf{D}) &= (\mathbf{A} \cdot \mathbf{C})(\mathbf{B} \cdot \mathbf{D}) \\ - (\mathbf{A} \cdot \mathbf{D})(\mathbf{B} \cdot \mathbf{C}). \end{aligned} \quad (36)$$

The governing equation of ground water flow, has to be expressed in non-orthogonal, curvilinear coordinates. The hydraulic conductivity tensor can be expressed

$$\underline{\mathbf{K}} = \sum_i \sum_j K_{ij} \delta_i \delta_j = \sum_m \sum_n \kappa^{mn} \mathbf{g}_m \mathbf{g}_n. \quad (37)$$

Performing an inner (dot) product of the contravariant base vector for generalized curvilinear coordinates, \mathbf{g}^l , and Eq.(37)yields

$$\sum_i \sum_j K_{ij} \delta_i \delta_j \cdot \mathbf{g}^l = \sum_m \sum_n \kappa^{mn} \mathbf{g}_m \mathbf{g}_n \cdot \mathbf{g}^l = \sum_m \sum_n \kappa^{mn} \mathbf{g}_m \delta_n^l = \sum_m \kappa^{ml} \mathbf{g}_m. \quad (38)$$

Performing an inner (dot) product of Eq. (38) with \mathbf{g}^n gives

$$\kappa^{nl} = \sum_i \sum_j K_{ij} \delta_i \delta_j \cdot \mathbf{g}^l \cdot \mathbf{g}^n. \quad (39)$$

Using the definition of the contravariant base vectors (Eq.(31)),Eq.(39) can be written

$$\kappa^{nl} = \sum_i \sum_j K_{ij} \frac{\partial \xi^i}{\partial x_j} \frac{\partial \xi^n}{\partial x_i}. \quad (40)$$

Hence, in generalized curvilinear coordinates,

$$\underline{\mathbf{K}} = \sum_n \sum_l \sum_i \sum_j K_{ij} \frac{\partial \xi^i}{\partial x_j} \frac{\partial \xi^n}{\partial x_i} \mathbf{g}_n \mathbf{g}_l. \quad (41)$$

The hydraulic conductivity tensor has nine terms (only three terms when the coordinate axes are aligned with the principal axes of \mathbf{K} in Cartesian coordinates; extra terms are required in generalized curvilinear coordinates).

Conservative expressions for the gradient of a scalar, ϕ , and for the divergence of a vector, \mathbf{q} , in generalized curvilinear coordinates are

$$\nabla \phi = \frac{1}{\sqrt{g}} \sum_i \left[(\mathbf{g}_j \times \mathbf{g}_k) \phi \right]_{\xi^i} = \frac{1}{\sqrt{g}} \sum_i \left[\sqrt{g} \mathbf{g}^i \phi \right]_{\xi^i} \text{ and} \quad (42)$$

$$\nabla \cdot \mathbf{q} = \frac{1}{\sqrt{g}} \sum_i \left[(\mathbf{g}_j \times \mathbf{g}_k) \cdot \mathbf{q} \right]_{\xi^i} = \frac{1}{\sqrt{g}} \sum_i \left[\sqrt{g} \mathbf{g}^i \cdot \mathbf{q} \right]_{\xi^i}. \quad (43)$$

Eqs.(42) and (43) can be approximated by non-conservative expressions,

$$\nabla \phi = \frac{1}{\sqrt{g}} \sum_i (\mathbf{g}_j \times \mathbf{g}_k) \phi_{\xi^i} = \sum_i \mathbf{g}^i \phi_{\xi^i} \text{ and} \quad (44)$$

$$\nabla \cdot \mathbf{q} = \frac{1}{\sqrt{g}} \sum_i (\mathbf{g}_j \times \mathbf{g}_k) \cdot \mathbf{q}_{\xi^i} = \sum_i \mathbf{g}^i \cdot \mathbf{q}_{\xi^i}, \quad (45)$$

as

$$\sum_i (\mathbf{g}_j \times \mathbf{g}_k)_{\xi^i} = 0 \quad (46)$$

Thompson et al. (1985) state" ... the quantity $(\mathbf{g}_j \times \mathbf{g}_k)$ represents an increment of surface area, so that $[(\mathbf{g}_j \times \mathbf{g}_k) \cdot \mathbf{q}]$ is a flux through this area. It is clear that the difference between the two forms is that the area used in the numerical representation of the flux in the conservative form, Eq. (43), is the area of the individual sides of the volume element, but in the non-conservative form, Eq. (45), a common area evaluated at the center of the volume element is used."

The non-conservative form of Darcy's law

$$\mathbf{q} = -\nabla \cdot (\underline{\mathbf{K}} \cdot \nabla \phi)$$

using Eqs. (41) and (44), becomes

$$\begin{aligned} \mathbf{q} &= -\sum_n \sum_l \sum_i \sum_j \sum_m K_{ij} \frac{\partial \xi^i}{\partial x_j} \frac{\partial \xi^n}{\partial x_i} \mathbf{g}_n \mathbf{g}_l \cdot \mathbf{g}^m \phi_{\xi^m} \\ &= -\sum_n \sum_l \sum_i \sum_j K_{ij} \frac{\partial \xi^i}{\partial x_j} \frac{\partial \xi^n}{\partial x_i} \mathbf{g}_n \phi_{\xi^l}, \end{aligned} \quad (47)$$

using Eq. (32b). Substituting Eq. (47) into Eq. (45)

$$\text{gives } \nabla \cdot \mathbf{q} = -\sum_n \sum_l \sum_i \sum_j \sum_m \mathbf{g}^m \cdot \left(K_{ij} \frac{\partial \xi^i}{\partial x_j} \frac{\partial \xi^n}{\partial x_i} \mathbf{g}_n \phi_{\xi^l} \right)_{\xi^m} \quad (48)$$

Expanding Eq. (48) into three terms and using the continuity equation gives

$$\begin{aligned} \nabla \cdot \mathbf{q} &= -\sum_n \sum_l \sum_i \sum_j \sum_m K_{ij} \frac{\partial \xi^i}{\partial x_j} \frac{\partial \xi^n}{\partial x_i} \mathbf{g}^m \cdot \mathbf{g}_n \phi_{\xi^l} \xi^m \\ &\quad - \sum_n \sum_l \sum_i \sum_j \sum_m K_{ij} \left(\frac{\partial \xi^i}{\partial x_j} \frac{\partial \xi^n}{\partial x_i} \right)_{\xi^m} \mathbf{g}^m \cdot \mathbf{g}_n \phi_{\xi^l} \\ &\quad - \sum_n \sum_l \sum_i \sum_j \sum_m K_{ij} \frac{\partial \xi^i}{\partial x_j} \frac{\partial \xi^n}{\partial x_i} \mathbf{g}^m \cdot (\mathbf{g}_n)_{\xi^m} \phi_{\xi^l} = 0 \end{aligned} \quad (49)$$

Eq. (49)uses $(\mathbf{K}_{ij})_{\xi^m} = 0$; this condition assumes that the hydraulic conductivity tensor inside an element is constant. Using Eq. (32a), Eq. (49)reduces to

$$\begin{aligned} &\sum_n \sum_l \sum_i \sum_j K_{ij} \frac{\partial \xi^i}{\partial x_j} \frac{\partial \xi^n}{\partial x_i} \phi_{\xi^l} \xi^n \\ &+ \sum_n \sum_l \sum_i \sum_j K_{ij} \left(\frac{\partial \xi^i}{\partial x_j} \frac{\partial \xi^n}{\partial x_i} \right)_{\xi^n} \phi_{\xi^l} \\ &+ \sum_n \sum_l \sum_i \sum_j \sum_m K_{ij} \frac{\partial \xi^i}{\partial x_j} \frac{\partial \xi^n}{\partial x_i} \mathbf{g}^m \cdot (\mathbf{g}_n)_{\xi^m} \phi_{\xi^l} = 0. \end{aligned} \quad (50)$$

Eq. (50) is a non-conservative form of the equation governing ground water flow in generalized curvilinear coordinates. If the curvilinear coordinates (ξ^i) are the

same as Cartesian coordinates, Eq. (50) simplifies so that only the first term stays. The second term expresses the stretching of the curvilinear coordinates. The third term expresses the rotation and/or angular deformation of the curvilinear coordinates. The covariant and contravariant base vectors are different in different cells. The third term can also be expressed by a control function of EAGLE (Thompson et al., 1985), which will not be discussed here. Expansion of the third term requires the Christoffel tensor, which defines derivatives of covariant and contravariant base vectors; hence,

$$\frac{\partial}{\partial \xi^j} g_i = \sum_k \Gamma_{ij}^k g_k \quad \text{and} \quad (51a)$$

$$\frac{\partial}{\partial \xi^j} g^i = -\sum_k \Gamma_{kj}^i g^k, \quad (51b)$$

where Γ_{ij}^k is the Christoffel tensor and can be written

$$\Gamma_{ij}^k = \frac{1}{2} \sum_l g^{kl} \left(\frac{\partial g_{il}}{\partial \xi^j} + \frac{\partial g_{jl}}{\partial \xi^i} - \frac{\partial g_{ij}}{\partial \xi^l} \right) \quad (52)$$

Eq. (50) becomes

$$\begin{aligned} & \sum_n \sum_l \sum_i \sum_j K_{ij} \frac{\partial \xi^l}{\partial x_j} \frac{\partial \xi^n}{\partial x_i} \phi_{\xi^l \xi^n} \\ & + \sum_n \sum_l \sum_i \sum_j K_{ij} \left(\frac{\partial \xi^l}{\partial x_j} \frac{\partial \xi^n}{\partial x_i} \right)_{\xi^k} \phi_{\xi^l} \\ & + \sum_n \sum_l \sum_i \sum_j K_{ij} \frac{\partial \xi^l}{\partial x_j} \frac{\partial \xi^n}{\partial x_i} \Gamma_{nm}^m \phi_{\xi^l} = 0. \end{aligned} \quad (53)$$

Eq. (53) needs to be modified for numerical implementation as the coefficient of the second term is not based upon ξ^i . Another expression can be stated by starting the hydraulic conductivity to be expressed by the contravariant base vectors by the definition of the covariant base vectors (Eq. 30), so that

$$\underline{K} = \sum_n \sum_l \sum_i \sum_j K_{ij} \frac{\partial x_j}{\partial \xi^l} \frac{\partial x_i}{\partial \xi^n} g^n g^l. \quad (54)$$

Following the previous procedure, the governing equation can be expressed as

$$\begin{aligned} & \sum_k \sum_m \sum_n \sum_l \sum_j K_{ij} \frac{\partial x_j}{\partial \xi^l} \frac{\partial x_i}{\partial \xi^n} g^{lm} g^k \cdot (g^n)_{\xi^k} \phi_{\xi^m} \\ & + \sum_k \sum_m \sum_n \sum_l \sum_j K_{ij} g^{lm} g^{kn} \left(\frac{\partial x_j}{\partial \xi^l} \frac{\partial x_i}{\partial \xi^n} \right)_{\xi^k} \phi_{\xi^m} \\ & + \sum_k \sum_m \sum_n \sum_l \sum_j K_{ij} \frac{\partial x_j}{\partial \xi^l} \frac{\partial x_i}{\partial \xi^n} g^{kn} (g^{lm})_{\xi^k} \phi_{\xi^m} \\ & + \sum_k \sum_m \sum_n \sum_l \sum_j K_{ij} \frac{\partial x_j}{\partial \xi^l} \frac{\partial x_i}{\partial \xi^n} g^{kn} g^{lm} \phi_{\xi^m \xi^k} = 0. \end{aligned} \quad (55a)$$

Apply the Christoffel tensor on the first term of Eq.

(55a), the governing equation becomes

$$\begin{aligned} & -\sum_k \sum_m \sum_n \sum_l \sum_j \sum_i K_{ij} \frac{\partial x_j}{\partial \xi^l} \frac{\partial x_i}{\partial \xi^n} g^{lm} g^{k'k} \Gamma_{k'k}^n \phi_{\xi^m} \\ & + \sum_k \sum_m \sum_n \sum_l \sum_j \sum_i K_{ij} g^{lm} g^{kn} \left(\frac{\partial x_j}{\partial \xi^l} \frac{\partial x_i}{\partial \xi^n} \right)_{\xi^k} \phi_{\xi^m} \\ & + \sum_k \sum_m \sum_n \sum_l \sum_j \sum_i K_{ij} \frac{\partial x_j}{\partial \xi^l} \frac{\partial x_i}{\partial \xi^n} g^{kn} (g^{lm})_{\xi^k} \phi_{\xi^m} \\ & + \sum_k \sum_m \sum_n \sum_l \sum_j \sum_i K_{ij} \frac{\partial x_j}{\partial \xi^l} \frac{\partial x_i}{\partial \xi^n} g^{kn} g^{lm} \phi_{\xi^m \xi^k} = 0. \end{aligned} \quad (55b)$$

Eq. (55b) is used for numerical implementation as all terms are based on the generalized curvilinear coordinates (ξ^i).

4.2 Free surface boundary condition

The free surface location is determined by the recharge rate, hydraulic conductivity, and the effective porosity of the porous medium for the unsteady state problem. The free surface boundary condition in the Cartesian coordinates is

$$\frac{\partial F}{\partial t} + \left(\frac{q - N}{n_e} \right) \cdot \nabla F = 0, \quad (56)$$

N =vertical recharge and F is the function represents the free function.

4.2.1 Steady state

The recharge rate in Cartesian and curvilinear coordinates is

$$\underline{N} = \sum_i N_i \delta_i = \sum_j N_j g^j = \sum_i \sum_j N_i \frac{\partial \xi^j}{\partial x_i} g_j \quad (57)$$

The normal vector, ∇F , of any surface can be easily approximated numerically, is

$$\nabla F = \sum_i F_{x_i} \delta_i = \sum_i \sum_j F_{x_i} \frac{\partial x_i}{\partial \xi^j} g^j \quad (58)$$

Substituting Eqs.(47),(57) and (58) into Eq. (56) gives

$$\begin{aligned} & \left(-\sum_n \sum_l \sum_i \sum_j K_{ij} \frac{\partial \xi^l}{\partial x_j} \frac{\partial \xi^n}{\partial x_i} g^n \phi_{\xi^l} - \sum_i \sum_j N_i \frac{\partial \xi^j}{\partial x_i} g_j \right) \\ & \cdot \sum_m \sum_k F_{x_m} \frac{\partial x_m}{\partial \xi^k} g^k \end{aligned} \quad (59)$$

which can be condensed as

$$\begin{aligned} & -\sum_m \sum_l \sum_i \sum_j \sum_k K_{ij} F_{x_m} \frac{\partial x_m}{\partial \xi^k} \frac{\partial \xi^l}{\partial x_j} \frac{\partial \xi^n}{\partial x_i} \phi_{\xi^l} \\ & - \sum_i \sum_k \sum_m N_i F_{x_m} \frac{\partial x_m}{\partial \xi^k} \frac{\partial \xi^k}{\partial x_i} = 0 \end{aligned} \quad (60)$$

4.2.2 Unsteady-state

The three-dimensional unsteady state free surface

boundary condition can be expressed in Cartesian coordinates, from Eq. (56), as

$$\frac{\partial \phi}{\partial t} - \frac{1}{n_e} \left[K_{xx} \left(\frac{\partial \phi}{\partial x} \right)^2 + K_{yy} \left(\frac{\partial \phi}{\partial y} \right)^2 + K_{zz} \left(\frac{\partial \phi}{\partial z} \right)^2 - \frac{\partial \phi}{\partial z} (K_{zz} + N) + N \right] = 0. \quad (61)$$

The unsteady free surface boundary condition in generalized curvilinear coordinates is obtained by applying the chain rule and substituting Eqs. (7) into Eq. (61). The two-dimensional form is

$$\frac{\partial \phi}{\partial t} n_e = K_{xx} \left(\frac{y_{\eta}^2}{g} \phi_{\xi}^2 - \frac{2y_{\eta}y_{\xi}}{g} \phi_{\eta} \phi_{\xi} + \frac{y_{\xi}^2}{g} \phi_{\eta}^2 \right) + K_{yy} \left(\frac{x_{\eta}^2}{g} \phi_{\xi}^2 - \frac{2x_{\eta}x_{\xi}}{g} \phi_{\eta} \phi_{\xi} + \frac{x_{\xi}^2}{g} \phi_{\eta}^2 \right) - \left(-\frac{x_{\eta}}{\sqrt{g}} \phi_{\xi} + \frac{x_{\xi}}{\sqrt{g}} \phi_{\eta} \right) (K_{yy} + N) + N. \quad (62)$$

5. Conclusions

Estimation of free surface and ground water mounding can be computed in the Cartesian coordinates. The major disadvantages are the accuracy depending upon the grid size and the changing of the flow domain. Application of generalized curvilinear coordinates simplifies the estimation of the free and moving boundary because the free and moving boundary locates on the grid points. However, this method introduces truncation error. This paper derived a complete tensor form of poisson type equation in the curvilinear coordinates, which included a control function in EAGLE. This complete form satisfies any grid generated by any grid generator. The computation code is available on request.

Bibliography

1. Aris, R. Vectors, Tensor, and the Basic Equations of Fluid Mechanics Prentice-Hall, Inc., 286 pages, 1962.
2. Bird, R. B.; Armstrong, R.C. and Hassager, O. Dynamics of Polymeric Mechanics, Volume 1, Fluid Mechanics New York: John Wiley & Sons, 649 pages. 1987.
3. Brock, R. R. "Dupuit-Forchheimer and potential theories for recharge from basins," Water Resources Research 12(5), 1976, pp.909-911.
4. Dagan, G. "Linearized solutions of free-surface groundwater flow with uniform recharge," Journal of Geophysical Research 72(4, Feb.), 1967, pp. 1183-1193.
5. Fletcher, C.A.J. Computational Techniques for Fluid Dynamics. New York: Springer-Verlag, 493 pages. 1991.
6. Grinskii, N.K. "Complex potential of flow with free surface in a stratum of relatively small thickness and $k=f(z)$," (in Russian). Dokl. Akad. Nauk SSSR 51(5), 1964, pp. 337-338.
7. Haar, M. E. Ground Water and Seepage. New York: McGraw-Hill Book Co. Inc. 1962.
8. Hantush, M. S. "Growth and decay of groundwater-mounds in response to uniform percolation," Water Resources Research 3(1), 1967, pp. 227-234.
9. Huisman, L. Ground-Water Recovery. New York: Winchester Press, 1972.
10. Kirkham, D. and Powers, W.L. "An exact theory of seepage of steady rainfall into tile and ditch drained land of finite depth," 8th Intern. Congress of Soil Science, Bucharest, Romania, 1964, 39-44.
11. Lennon, G. P.; Liu, P.L-F and Liggett, J.A. "Boundary integral solutions to three-dimensional unconfined Darcy's flow," Water Resources Research 16(4, August), 1980, pp. 651-658.
12. Liggett, J. A. and Hadjitheodorou, C. "Initial motion problem in porous media," Journal of the Hydraulics Division, Proceedings of the ASCE HY3, 1965, pp. 61-81.
13. Liggett, J.A. "Location of free surface in porous media," Journal of the Hydraulics Division, Proceedings of the ASCE HY4 (April), 1977, pp. 353-365.
14. Liu, P.L-F and Liggett, J.A. "Boundary solutions to two problems in porous media," Journal of the Hydraulics Division, Proceedings of the ASCE HY3 (March), 1979, pp. 171-183.
15. Maasland, D.E.L. and Bittinger, M. W. Proceeding of the Symposium of Transient Ground Water Hydraulics. Civil Engineering Section, Colorado State University, Fort Collins, CO., 1963.

16. McDonald, M. G. and Harbaugh, A. W. A Modular Three-dimensional Finite-Difference Ground-Water Flow Model. Washington, D. C., Science Software Group, Techniques of Water-Resources Investigations of the United States Geological Survey, 1988.

17. Thompson, J. E.; Warsi, Z.U.A. and Mastin, C. W. (Eds.) Numerical Grid Generation-Foundations and Applications. New York: North-Holland, 483 pages., 1985.

收稿日期：民國 84 年 8 月 20 日

接受日期：民國 84 年 9 月 12 日

(上接第85頁)

three bubbles of 0.99 cm/sec. The bubbles appeared to be moving in the center of the spacing, which is the maximum velocity. 2/3 of this velocity (0.66 cm/sec) is in good agreement with the average velocity, which is equal to $K_m = 0.69$ cm/sec.

6.3 Conclusions

The Hele-Shaw model is a very useful device for visualizing unconfined, ground water flows, as the free surface can be easily observed. From the analog relation, the simulated hydraulic conductivity is proportional to the square of the spacing. The spacing of this model is the most difficult parameter to be controlled and to be measured. The spacing of the Hele-Shaw model is not uniform. It ranged from 0.109 inch to 0.119 inch for the portion tested.

Numerical and experimental results are in good agreement for the homogeneous aquifer. The maximum height of mounding could not be observed when the recharge rate was equal to the simulated hydraulic conductivity as the area under the recharge was filled with oil. An important condition in this saturated region is that there is no horizontal flow only vertical flow due to gravity. Once flow passes through the free surface, horizontal flow begins.

Bibliography

- Bear, J. Dynamics of Fluids in Porous Media. New York: Dover Publication, Inc., 764 pages, 1972.
- Harr, M. E. Ground Water and Seepage, New York: McGraw-Hill Book Co. Inc. 1962.
- Murray, W. A. Seepage Face Effects in Unsteady Ground-water Flow. Ph. D. Thesis, Civil and Environmental Engineering, University of Wisconsin at Madison, 1970.
- Polubarinava-Kochina, P. Ya. Theory of Ground Water Movement. Translated by J. DeWiest, Princeton: Princeton University Press, 1962.
- Schlichting, H. Boundary Layer Theory. 7th Ed. Translated by J. Kestin, New York: McGraw-Hill, 1979.

收稿日期：民國 84 年 8 月 20 日

接受日期：民國 84 年 9 月 12 日